Anal. Bioanal. Electrochem., Vol. 16, No. 6, 2024, 559-567
https://www.doi.org/10.22034/abec.2024.714079

Analytical & Bioanalytical Electrochemistry

Full Paper

Electrochemical Investigation of The Inhibitory Effect of Zinc Oxide Nanoparticles/Tenofovir Disoproxil Fumarate Nanocomposite on Mild Steel Corrosion in 1 M Hydrochloric Acid

Msenhemba Moses Mchihi,[1,*] Nnenna Winifred Odozi,[2] and Shittu Alhameen Gbolahan[3]

[1]*Department of Chemical Science, School of Science, Yaba College of Technology Lagos, Nigeria*
[2]*Department of Chemistry, Faculty of Science, University of Ibadan, Nigeria*
[3]*Department of Science Education, School of Technical Education, Yaba College of Technology Lagos, Nigeria*

*Corresponding Author, Tel.: +234 8060123864
E-Mails: mosesmsenhemba@gmail.com and msenhemba.mchihi@yabatech.edu.ng

Received: 12 January 2024 / Received in revised form: 22 June 2024 / Accepted: 24 June 2024 / Published online: 30 June 2024

Abstract- Corrosion of mild steel is a disturbing phenomenon that deserves effective measures to avert accidents, equipment breakdown, and economic downturns. The corrosion inhibitory potentials of zinc oxide nanoparticles/tenofovir disoproxil fumarate nanocomposite (Z+D) was investigated using potentiodynamic polarization (PDP) and electrochemical impedance spectroscopy (EIS). PDP analysis revealed that the alteration in corrosion potential values in the presence of Z+D (compared to corrosion potential obtained in the absence of Z+D) was less than 85 mV which suggest that Z+D operated as a mixed-type inhibitor. Corrosion current density (I_{corr}) decreased tremendously from 1241 μAcm^{-2} (in the absence of Z+D) to 321 μA cm^{-2} in the presence of 1000 ppm of the inhibitor. The inhibition efficiency increased with an increase in concentration of inhibitor to reach 74% when 1000 ppm of the inhibitor was introduced. EIS studies revealed a tremendous increase in charge transfer resistance (R_{ct}) from 3533 Ω cm^2 (in the absence of the inhibitor) to 21464×cm^2 when 1000 ppm of Z+D was introduced. The highest inhibition efficiency (i.e 84%) computed from EIS analysis was obtained when 1000 ppm of the inhibitor was introduced. Electrochemical findings suggest that Z+D exhibited good attributes as a corrosion inhibitor for mild steel in 1 M hydrochloric acid.

Keywords- Corrosion inhibitor; Tenofovir disoproxil fumarate; Mild steel; Acid; nanocomposite; Electrochemical study

1. INTRODUCTION

The use of acid solutions for cleaning operations on mild steel in various industries (especially oil and gas industries) often results to deterioration of mild steel which is popularly known as corrosion [1-5]. Corrosion of metals has caused enormous environmental and economic problems globally. Owing to the numerous problems associated with metallic corrosion, researchers have developed numerous techniques for corrosion mitigation in diverse media. The use of inhibitors for corrosion mitigation is economical and simple compared to other techniques such as cathodic protection and sacrificial coatings. Corrosion inhibitors that consist of groups capable of establishing chemical links with the surface of the metal via the transfer of electrons are known to be efficient [6]. The metal functions as an electrophile while the inhibitor act as Lewis base, whose electrons are utilized for formation of a bond. The inhibitory efficacy of several compounds for mild steel corrosion in diverse media has been reported. However, some of the studied compounds are highly toxic and are capable of causing environmental problems. In addition, some of the corrosion inhibitors are scarce or require scarce chemicals for their synthesis.

The use of nanomaterials as inhibitors of corrosion is currently receiving tremendous attention owing to their high surface-to-volume ratio. The use of zinc oxide nanoparticles (ZnONPs) as inhibitors for mild steel corrosion in an acidic medium has been reported. Zinc oxide is chemically stable. It is also known to have high thermal stability. The high surface area of zinc oxide nanoparticles compared with their bulk counterpart could also favor their use as corrosion inhibitors owing to increase in surface coverage [7]. However, agglomeration tendency (owing to their high specific area and strong interparticle interactions) is one drawback associated with the use of metal oxide nanoparticles [8]. One way to overcome this challenge is via functionalization or mere compositing with other compounds with interesting functionalities like tenofovir disoproxil fumarate [8]. The efficacy of metal oxide-based nanocomposites has been reported [8-10]. Aslam et al. (2022) [8] employed zirconium oxide-glycine nanocomposite as an inhibitor for mild steel corrosion in hydrochloric acid [8]. The zirconium oxide-glycine nanocomposite utilized by the researchers exhibited mixed-type behavior and 81 % inhibition efficiency was achieved when 500 ppm was introduced at 343 K [8]. An upsurge of inhibition efficiency was also recorded by Aslam et al. (2022) with a rise in concentration of zirconium oxide-glycine nanocomposite. Similarly, Quadri et al (2017) [9] reported the utilization of three different nanocomposites of ZnONPs with different polymers as acid-induced corrosion inhibitors for mild steel. All three nanocomposites exhibited mixed-type attributes. Between 58-80 % inhibition efficiency was achieved upon introduction of each of the three nanocomposites in the corrosive medium [9].

Tenofovir disoproxil fumarate (TDF) is a popular drug that is known for its efficacy in inhibiting retroviruses activity (i.e an antiretroviral). More precisely, it is employed for the treatment of viral conditions such as acquired immune deficiency syndrome (AIDS) and viral

hepatitis. It functions as an inhibitor of nucleoside analogue reverse transcriptase and was fashioned to enhance permeability and absorption [11]. The molecular formula for TDF is $C_{23}H_{34}N_5O_{14}P$ which clearly indicates its wealth of hetero atoms. The presence of hetero atoms such as P, O, and N which are capable of supplying electrons to vacant d orbitals of iron is an important attribute for excellent inhibitors of corrosion. Therefore, this study was designed to investigate the efficacy of a mixture of zinc oxide nanoparticles and tenofovir disoproxil fumarate as corrosion inhibitors for mild steel in a hydrochloric acid medium. To the best of our knowledge, this has not been reported.

2. EXPERIMENTAL METHODS

2.1. Preparation of Specimen

The tenofovir disoproxil fumarate (mylan) employed for this study was obtained at Serge Pharmcacy, along Lagos University Teaching Hospital road, Surulere, Lagos. 1.6 g of tenofovir disoproxil fumarate tablets were pulverized to obtain a powder that was mixed with 1.6 g of zinc oxide nanoparticles (i.e in the ratio of 1:1) to obtain ZnONPs/ tenofovir disoproxil fumarate nanocomposite abbreviated as Z+D. The corrosive 1 M HCl employed in this study was prepared by diluting an appropriate volume of 37% HCl (analytical grade) using an appropriate volume of double distilled water. 500 ppm and 1000 ppm of the inhibitor (Z+D) solution in the HCl medium were subsequently prepared using the 1 M HCl. A mild steel sheet comprising 98.835 Fe, 0.13 C, 0.18 Si, 0.39 Mn, 0.40 P, 0.04 S, and Cu 0.025 (all in wt.%) was purchased in portharcourt, Rivers state Nigeria and utilized for this study.

2.2. Electrochemical studies

A cell assembly comprising platinum wire as counter electrode, 1 cm^2 exposed mild steel surface as working electrode, and Ag/AgCl as reference electrode, together with Metrohm Autolab PGSTAT204 Potentiostat/Galvanostat was employed for electrochemical measurements (at room temperature). The reported potentials in this report are vs. Ag/AgCl. It is important to mention that the platinum wire was employed to specifically complete the circuit. The free dissolution potential of mild steel specimens was determined prior to other electrochemical experiments by obtaining the open circuit potential (OCP) for 30 minutes to ensure a system that is devoid of instability and reduces the influence of charging current [9,10]. Electrochemical impedance spectroscopic (EIS) tests were executed between 100 kHz to 10 mHz (i.e frequency range) and signal amplitude perturbation of 10 mV. Hydrochloric acid was utilized as the electrolyte for this investigation. Charge transfer resistance (R_{ct}) values obtained from EIS were used to compute percentage inhibition efficiency (IE) with the aid of equation 1.

$$\%IE = \frac{Rct - R°ct}{Rct} X\ 100 \quad (1)$$

Where R_{ct}=Resistance to charge transfer in the presence of Z+D, R^0_{ct}=Resistance to charge transfer in the absence of Z+D.

Potentiodynamic polarization **(**PDP) tests were executed between -250 mV and +250 mV (potential range), while the OCP scanning rate was set at 0.2 mV/s. The data obtained was analyzed using electrochemical analytical softwares such as Zsimpwin 3.2 model and EC-lab for EIS and PDP respectively. Equation 2 was employed to calculate the IE for PDP.

$$\%IE = \frac{I°corr - Icorr}{i°corr} X\ 100 \quad (2)$$

Where I°corr = corrosion current density in the absence of Z+D, I_{corr}=corrosion current density in the presence of Z+D. Equation 3 was employed to calculate the surface coverage (θ).

$$\theta = IE \div 100 \quad (3)$$

3. RESULTS AND DISCUSSION

3.1. Open circuit potential (OCP)

The OCP-time profiles for mild steel in 1 M HCl devoid of Z+D and in the presence of 500 ppm and 1000 ppm Z+D are presented in Figure 1. A substantial change was observed in OCP-time plots for mild steel in the presence of Z+D compared to the OCP versus time plot obtained in 1 M HCl devoid of Z+D. OCP values in the presence of Z+D shifted toward anodic direction (i.e towards more positive values) compared to the uninhibited HCl [10]. This suggest that, in 1 M HCl, Z+D has an influence on corrosion of mild steel [9]. Secondly, the observation also suggest that mild steel became nobler when Z+D was introduced in 1 M HCl [9].

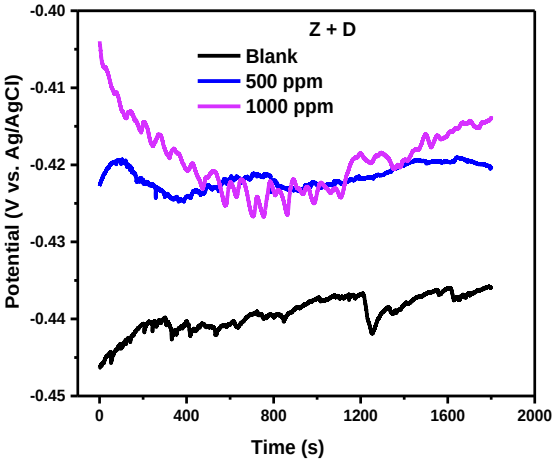

Figure 1. OCP-time plots for mild steel in 1 M HCl without and in the presence of Z+D

3.2. Potentiodynamic polarization studies (PDP)

Tafel plots for mild steel in 1 M HCl devoid of Z+D and in the presence of 500 ppm and 1000 ppm Z+D are presented in Figure 2. PDP findings revealed that the introduction of Z+D

into the corrosive medium decreased corrosion current densities [9,12]. That is, substantial decline in corrosion current density (I_{corr}) was observed in the presence of Z+D compared to values of I^{o}_{corr} as presented in Table 1. This remarkable decrease in I_{corr} in the presence of Z+D is a function of concentration (i.e I_{corr} value obtained when 1000 ppm of the inhibitor was introduced is less than I_{corr} value obtained when 500 ppm of the inhibitor was introduced). Consequently, inhibition efficiency equal to 74% was obtained (when 1000 ppm of inhibitor was introduced) which is greater than 61% obtained when 500 ppm of the inhibitor was introduced. This observed upsurge in %IE and θ with an upsurge in Z+D concentration could be as a result of increase in number of adsorbed Z+D molecules on the surface of mild steel. This observation is consistent with other reports in the literature [13-18].

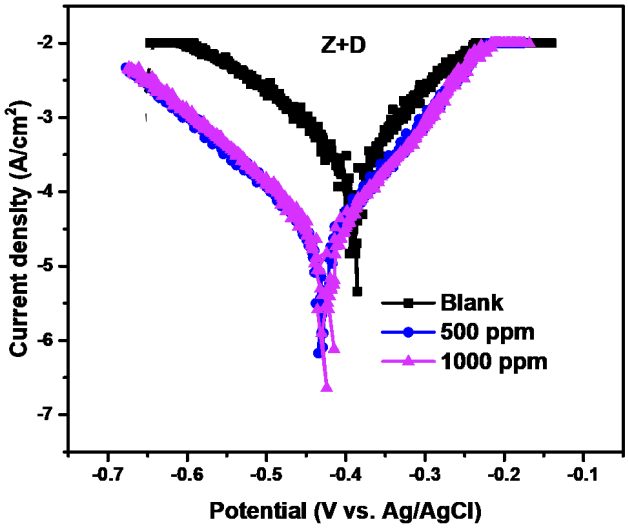

Figure 2. Potentiodynamic polarization plots for mild steel in 1 M HCl devoid of Z+D and in the presence of Z+D

Table 1. Parameters obtained from PDP studies for mild steel in 1 M HCl without and in the presence of Z+D

System	E_{corr} mV/SCE	I_{corr} μAcm^{-2}	βa mVdec^{-1}	βc mVdec^{-1}	θ	IE %
Blank	-421	1241	64	92		
500 ppm	-425	487	72	77	0.61	61
1000 ppm	-445	321	74	62	0.74	74

The introduction of 500 ppm and 1000 ppm of Z+D resulted in a shift of corrosion potential (E_{corr}) that is < 85 mV, suggesting that Z+D exhibited mixed-type inhibitor inclination. This observation is in agreement with Aslam et al. (2022) [9]. However, it is important to observe that Z+D displaced the E_{corr} cathodically. This suggests that even though Z+D showed mixed-

type propensity, Z+D reduces the dissolution of mild steel at the cathode better than at the anode [9]. Only a slight change was observed in cathodic Tafel slope (βc) and anodic Tafel slope (βa) values obtained in the presence and absence of Z+D. This suggests that the adsorption of Z+D on mild steel in the corrosive medium was via a geometric blocking mechanism [9].

3.3. Electrochemical impedance spectroscopy studies

Impedance plots (also called Nyquist plots) for mild steel in 1 M HCl devoid of Z+D and in the presence of Z+D are presented in Figure 3, while the associated parameters are presented in Table 2. The EIS spectra consist of semicircles that are imperfect. This imperfection could be due to differences in frequency dispersion typical of solid working electrodes or heterogeneity of the electrochemical system arising from impurities, surface unevenness, and the formation of porous inhibitor layers [12].

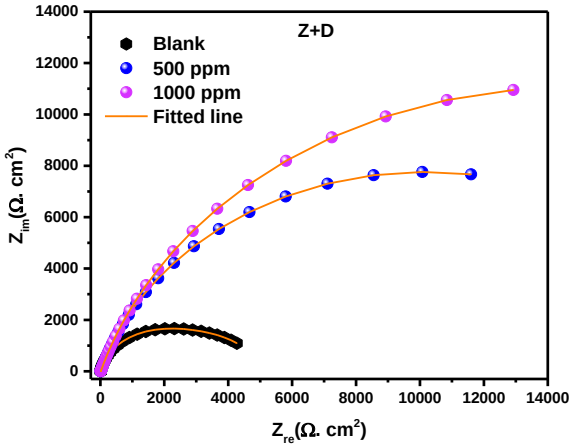

Figure 3. Nyquist plots for mild steel in 1 M HCl devoid of Z+D and in the presence of Z+D

Another important deduction from the Nyquist plots is the difference in the size of the semicircle obtained in HCl devoid of Z+D and in the presence of Z+D. A smaller semicircle diameter was observed in HCl devoid of Z+D compared to the diameter of the semicircle obtained in the presence of the Z+D. An upsurge in the diameter of the semicircle with the upsurge in Z+D concentration was observed which could be attributed to a rise in adsorbed Z+D molecules that are responsible for protective film formation [19]. A two-time constant equivalent circuit was adopted for fitting EIS data and is presented in Figure 4. Rs symbolizes the resistance of the solution, *Rpo* is pore resistance, CPE is the constant phase element and R_{ct} retains its usual meaning [20]. The data revealed two capacitances that are non-ideal i.e CPE1 and CPE2 owing to surface heterogeneity between the mild steel and film. The degree of nearness to ideal capacitance by the CPEs is described by the dispersion coefficients $n1$ and $n2$.

Table 2. EIS parameters for mild steel devoid of Z+D and in the presence of Z+D (in 1 M HCl)

System	R_s (Ω cm^2)	R_{po} (Ω cm^2)	CPE1 ($\mu\Omega^{-1}$ s^n $cm^{-2}\times10^{-5}$)	n1	R_{ct} (Ω cm^2)	CPE2 ($\mu\Omega^{-1}$ s^n cm^{-2} X 10^{-5})	n2	θ	IE %
Blank	10.5	1392	5.35	0.89	3533	5.91	0.85		
500 ppm	10.40	1564	1.11	0.96	15364	6.04	0.83	0.77	77
1000 ppm	10.6	2461	6.14	0.99	21464	5.82	0.81	0.84	84

It is imperative to note that, CPE acts similar to an ideal capacitance of the interface and bears the unit μFcm^{-2} when n is =1 [21]. Tremendous increase in R_{ct} was observed when Z+D was introduced in the corrosive medium as presented in Table 2. This upsurge in R_{ct} was consistent with upsurge in Z+D concentration and is in agreement with other reports [22-25]. Consequently, inhibition efficiency improved with rise in Z+D concentration to reach 84 % when 1000 ppm of Z+D was introduced.

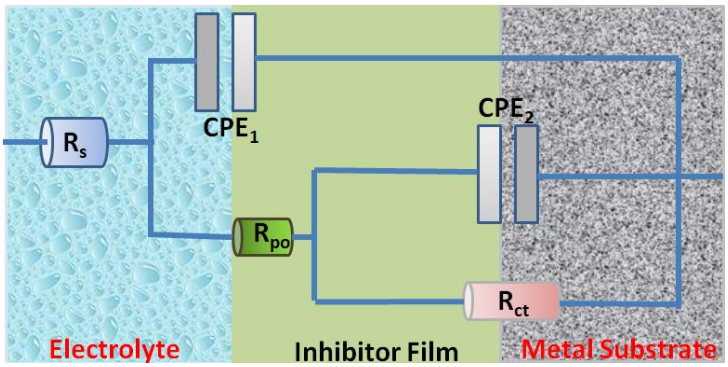

Figure 4. Two-time constant equivalent circuit for fitting EIS data

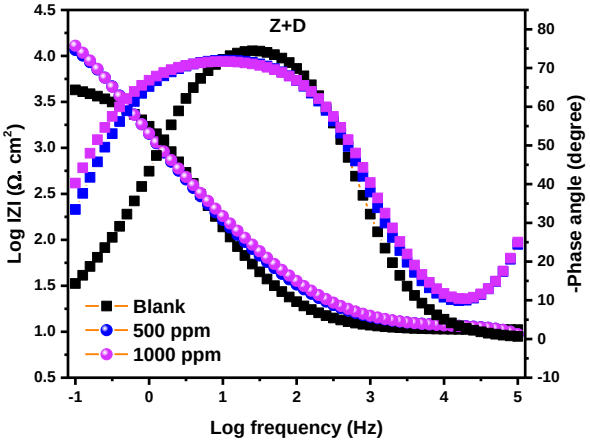

Figure 5. Bode and phase angle plots for mild steel in 1 M HCl without and in the presence of Z+D

Data presented in Table 2 revealed n less than 1 which suggest surface roughness and inhomogeneity. The Bode plots and phase angle plots for mild steel in 1 M HCl devoid of Z+D and in the presence of Z+D (Figure 5) showed an enlarged area under the curves in the presence of Z+D compared to the bare corrosive solution [19].

4. CONCLUSION

Potentiodynamic polarization studies revealed that ZnONPs/tenofovir disoproxil fumarate nanocomposite acted as a mixed-type inhibitor. A substantial decline in corrosion current density was observed in the presence of zinc oxide nanoparticles/tenofovir disoproxil fumarate nanocomposite compared to values of corrosion current density obtained in 1 M HCl without zinc oxide nanoparticles/tenofovir disoproxil fumarate nanocomposite. Charge transfer resistance increased tremendously when the inhibitor was introduced. Open circuit potential values for mild steel/1 M HCl system changed significantly in the presence of zinc oxide nanoparticles/tenofovir disoproxil fumarate nanocomposite. The inhibition efficiency of the inhibitor improved tremendously with an upsurge in the concentration of zinc oxide nanoparticles/tenofovir disoproxil fumarate nanocomposite. Zinc oxide nanoparticles/ tenofovir disoproxil fumarate nanocomposite exhibited good attributes as corrosion inhibitor for mild steel in 1 M hydrochloric acid.

Declarations of interest

The authors declare no conflict of interest in this reported work.

REFERENCES

[1] H. Elmsellem, T. Harit, A. Aouniti, F. Malek, A. Riahi, A. Chetouani, and B. Hammouti, Prot. Met. Phys. Chem. 51 (2015) 873.

[2] A. Khadiri, R. Saddik, K. Bekkouche, A. Aouniti, B. Hammouti, N. Benchat, M. Bouachrine, and R. Solmaz, J. Taiwan Inst. Chem. Eng. 58 (2016) 552.

[3] H. Elmsellem, A. Elyoussfi, H. Steli, N.K. Sebbar, E.M. Essassi, M. Dahmani, Y. El Ouadi, A. Aouniti, B. El Mahi, and B. Hammouti, Der Pharma Chem. 8 (2016) 248.

[4] K. Bouayad, Y. Kandri Rodi, E.H. El Ghadraoui, H. Elmsellem, Y. Ouzidan, B. El Mahi, E. M. Essassi, I. Abdel-Rahman, A. Chetouani, and B. Hammouti, Mor. J. Chem. 5 (2017) 285.

[5] S. Aourabi, M. Driouch, M. Kadiri, N. Achnine, M. Sfaira, F. Mahjoubi, M. Sfaira, B. Hammouti, and K.M. Emran, Arabian J. Chem. 13 (2021) 7183.

[6] K. Zaidi, C. Merimi, W. Daoudi, O. Dagdag, A. Berisha, A. Aouniti, A. Oussaid, R. Touzani, M. Messali, and B. Hammouti, Mor. J. Chem. 14 (2023) 411.

[7] H.R. Ghorbani, F.P. Mehr, H. Pazoki, and B.M. Rahmani, Orient. J. Chem. 32 (2015) 1219.
[8] R. Aslam, M. Mobin, and M. Shoeb, J. Aslam, Sci. Rep. 12 (2022) 9274.
[9] T.W. Quadri, L. O. Olasunkanmi, O. E. Fayemi, M. M. Solomon, and E.E. Ebenso, ACS Omega 2 (2017) 8421.
[10] A.M. Abdel-karim, Y.M. Ahmed, and M.M. El-Masry, Scientific Reports 13 (2023) 19248.
[11] G.C. Clososki, R.A. Soldi, R.M. da Silva, T. Guaratini, N.C. Lopes, R.R. Pereira, L.C. Lopes, T. dos Santos, R.B. Martins, C.S. Costa, A.N. de Carvalho, L.P. daSilva, E. Arruda, and N.P. Lopes, J. Braz. Chem. Soc. 31 (2020) 1552.
[12] A. Hbika, A. Bouyanzer, M. Jalal, N. Setti, E. Loukili, A. Aouniti, Y. Kerroum, I. Warad, B. Hammouti, and A. Zarrouk, Anal. Bioanal. Electrochem. 15 (2023) 17.
[13] F. Chioma, N.W. Odozi, M.M. Mchihi, and M.A. Olatunde, Global J. Pure Appl. Sci. 28 (2022).
[14] Y. Youssefi, L. Oucheikh, O. Ou-ani, M. Jabha, A. Oubair, M. Znini, and B. Hammouti, Mor. J. Chem. 14 (2023) 155.
[15] F. Yousfi, M. El Azzouzi, M. Ramdani, H. Elmsellem, A. Aouniti, N. Saidi, B. El Mahi, A. Chetouani, and B. Hammouti, Der Pharma Chem. 7 (2015) 377.
[16] G. Ijuo, H. Chahul, I. Eneji, J. Adv. Electrochem. 2 (2016) 107.
[17] M. Saadouni, M. Larouj, R. Salghi, H. Lgaz, S. Jodeh, M. Zougagh, and A. Souizi, Pharm. Lett. 8 (2016).
[18] D.K. Yadav, M.A. Quraishi, and B. Maiti, Corros. Sci. 55 (2012) 254.
[19] G.M. Al-Senani, Materials 13 (2020) 890.
[20] S. Aourabi, M. Driouch, M. Sfaira, F. Mahjoubi, B. Hammouti, C. Verma, E.E. Ebenso, and L. Guo, J. Mol. Liq. 323 (2021) 114950.
[21] V.I. Chukwuike, K. Rajalakshmi, and R.C. Barik, Appl. Surf. Sci. Adv. 4 (2021) 100079.
[22] N.W. Odozi, R. Saheed, and M.M. Mchihi, Chemsearch Journal 10 (2019) 88.
[23] M.M. Mchihi, A.M. Olatunde, N.W. Odozi, Mor. J. Chem. 12 (2024) 1122.
[24] J. Haque, M. A. Zulaikha, W. B. Wan Nik, D. Walid, E. Berdimurodov, and F. Zulkifli, Mor. J. Chem. 11 (2023) 1013.
[25] N.W. Odozi, A.S. Adetoba, M.M. Mchihi, and A.N. Akpaetok, ChemSearch Journal 12 (2021) 47.